ARTICLE   OPEN

Growth of In$_x$Ga$_{1-x}$Sb alloy semiconductor at the International Space Station (ISS) and comparison with terrestrial experiments

Y Inatomi[1,2,6], K Sakata[1], M Arivanandhan[3], G Rajesh[3], V Nirmal Kumar[3], T Koyama[3], Y Momose[3], T Ozawa[4], Y Okano[5,6] and Y Hayakawa[3,6]

BACKGROUND: In$_x$Ga$_{1-x}$Sb is an important material that has tunable properties in the infrared (IR) region and is suitable for IR-device applications. Since the quality of crystals relies on growth conditions, the growth process of alloy semiconductors can be examined better under microgravity (μG) conditions where convection is suppressed.
AIMS: To investigate the dissolution and growth process of In$_x$Ga$_{1-x}$Sb alloy semiconductors via a sandwiched structure of GaSb (seed)/InSb/GaSb(feed) under normal and μG conditions.
METHODS: In$_x$Ga$_{1-x}$Sb crystals were grown at the International Space Station (ISS) under μG conditions, and a similar experiment was conducted under terrestrial conditions (1G) using the vertical gradient freezing (VGF) method. The grown crystals were cut along the growth direction and its growth properties were studied. The indium composition and growth rate of grown crystals were calculated.
RESULTS: The shape of the growth interface was nearly flat under μG, whereas under 1G, it was highly concave with the initial seed interface being nearly flat and having facets at the peripheries. The quality of the μG crystals was better than that of the 1G samples, as the etch pit density was low in the μG sample. The growth rate was higher under μG compared with 1G. Moreover, the growth started at the peripheries under 1G, whereas it started throughout the seed interface under μG.
CONCLUSIONS: Kinetics played a dominant role under 1G. The suppressed convection under μG affected the dissolution and growth process of the In$_x$Ga$_{1-x}$Sb alloy semiconductor.

INTRODUCTION

In$_x$Ga$_{1-x}$Sb is a promising narrow-band-gap alloy semiconductor useful for numerous applications that demand high-quality crystals as substrate materials.[1–5] It has the advantage of having a tuneable lattice parameter and wavelength ranging from 6.096 to 6.479 and 1.7 to 6.8 μm by just adjusting its composition. However, it is difficult to grow high-quality In$_x$Ga$_{1-x}$Sb alloy bulk crystals because the solute and heat transport are influenced by convection, which affects the quality of the crystals.[6,7] Microgravity (μG) is an appropriate environment for investigating the solute transport and growth kinetics.[8,9] Under μG conditions, it is quite feasible to suppress the complex convective heat and mass transports to gain deeper insight into the transport phenomena. Also, materials science plays a vital part in mankind's efforts towards deeper space and planetary exploration.[10] The knowledge gained in the μG experiments can help to better understand and improve applications on Earth. In this respect, the role of gravity in the dissolution and growth mechanism of various materials, including narrow-band-gap semiconductors such as Ge, SiGe, GaSb and InSb, has been investigated for the past three decades.[11–16] Various physical factors such as granular convection, surface tension of liquid melts, dendritic growth velocities,

thermophysical properties of alloy melts, and phase separation in critical fluids have been examined in μG experiments.[17–21] We have also carried out several μG experiments using the space shuttle,[22] a drop tower[23] and a Chinese recoverable satellite.[24] The effect of diffusive transport and surface tension-induced Marangoni convection on the mixing of multi-component melts has been investigated using an In/GaSb/Sb sandwich sample.[25,26] Recently, the dissolution process and solute transport in a GaSb (seed)/InSb/GaSb (feed) sandwich sample were observed *in situ* using an X-ray penetration method under terrestrial conditions.[27] The results showed that gravity-induced solutal transport strongly influenced the dissolution process, and the numerical results clearly supported the experimental observations.[28] The above-mentioned results clearly suggest that convection affected not only the composition profiles but also the shape of the solid–liquid interface. Prior to the μG experiments at the International Space Station (ISS), preliminary experiments were carried out to optimize the growth conditions and measure various thermophysical properties of In$_x$Ga$_{1-x}$Sb alloy semiconductors.[29–31] The purpose of the 'Alloy Semiconductor' crystal growth project was to elucidate the factors affecting the crystal growth of a high-quality bulk ternary alloy semiconductor under μG conditions at the ISS.

[1]Institute of Space and Astronautical Science, Japan Aerospace Exploration Agency, Sagamihara, Japan; [2]School of Physical Sciences, SOKENDAI (The Graduate University for Advanced Studies), Sagamihara, Japan; [3]Research Institute of Electronics, Shizuoka University, Hamamatsu, Japan; [4]Department of Electrical Engineering, Shizuoka Institute of Science and Technology, Fukuroi, Japan and [5]Graduate School of Engineering Science, Osaka University, Toyonaka, Japan.
Correspondence: Y Inatomi (inatomi@isas.jaxa.jp)
[6]These authors contributed equally to this work.

This project was selected as one of the 14 candidate missions of the Kibo Second Phase Utilization in 2008. In the present article, we report our first μG experimental results for In$_x$Ga$_{1-x}$Sb alloy crystals grown at the ISS, and the results are compared with the terrestrial experiments.

MATERIALS AND METHODS

A GaSb(111)A/Te-doped InSb/GaSb(111)A sandwich sample was used for the growth of the In$_x$Ga$_{1-x}$Sb bulk crystal under μG at the ISS by the vertical gradient freezing method. GaSb single crystals along the <111> orientation were grown by the Czochralski method for the preparation of sandwich samples. Figure 1a–d shows a schematic diagram of the vertical temperature profile (a), initial stage of the sandwich sample (b), dissolution (c) and growth process (d) of the vertical gradient freezing method that was employed for the crystal growth. The ampoule with (GaSb(seed)/InSb/GaSb(feed)) sandwich sample was kept inside the furnace in which the temperature gradient was established (Figure 1a). During the high-temperature growth process, InSb was melted at its melting point of 525 °C. GaSb seed and feed crystals started to dissolve in InSb melt, and thereby InGaSb solution was formed (Figure 1c). Owing to the vertical temperature gradient, the solution at the seed interface gets super-saturated due to diffusive transport of solute from feed interface. Supersaturation provides the driving force to initiate the growth from un-dissolved seed crystal. Once crystal growth initiated at the seed
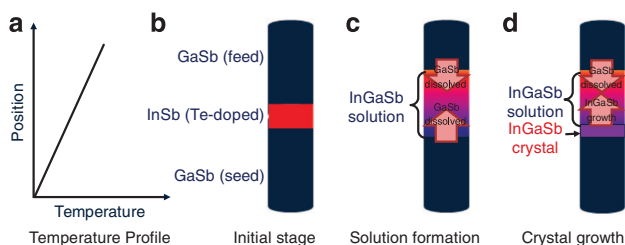
interface, seed dissolution was stopped and further growth was assisted by dissolution of feed crystal which is at relatively high temperature. Before the growth experiment, the temperature gradient of the furnace was calibrated at the ISS. The furnace was heated up to the reference temperature of 700 °C at a suitable heating rate (0.06 °C/min) after placing the growth ampoule in an appropriate position, and the temperature was kept constant for 107 h of growth. The temperature gradient in the furnace was fixed at 0.6 °C/mm. Based on the reference temperature (measured by the thermocouple) and the temperature gradient, the temperature at the GaSb seed interface was determined and controlled. To measure the growth rate of the crystal, several numbers of heat pulses were periodically introduced during the growth process after 3 h at 700 °C. To apply a heat pulse, the furnace temperature was increased by 10 °C from the growth temperature, held for 2 min and then cooled to the initial growth temperature. The increasing and decreasing times were fixed at 1 min and 10 s, respectively. By applying this kind of heat pulse, the Te impurity concentration was modulated and striations were introduced in the grown crystal. A total of 50 heat pulses were applied during the growth period at intervals of 2 h. For clear identification of the striations that are created by heat pulses, the introduction time interval between pulse number 4 and 5 was changed to 1 h. After applying all of the pulses, the temperature was decreased to 400 °C at a cooling rate of about 0.5 °C/min to reduce the thermal stress in the grown crystals. Then, the temperature was decreased to room temperature at a cooling rate of about 1 °C/min. A similar experiment was conducted under terrestrial conditions to study the effect of gravity on the dissolution and growth process (this sample is denoted the 1G sample). The grown crystals were cut along the growth direction and polished with alumina powder to obtain a mirrored surface. The polished sample was etched in a 1:3:1 solution of HF:KMnO$_4$:CH$_3$COOH for 30 min at room temperature to observe the Te impurity striations and etch pits. The composition profiles, interface shapes and striations of the grown crystals were analyzed by electron probe micro analysis (EPMA), polarized optical microscopy and field emission scanning electron microscopy.

For the numerical calculation, a two-dimensional symmetric rectangular model containing the GaSb seed and feed, an InSb melt, a boron nitride (BN) tube and a quartz tube was considered. In the simulation, the solution was assumed to be incompressible and Newtonian, and Boussinesq approximation was utilized. The Navier–Stokes and mass-continuity equations were used for the numerical analysis of the dissolution process. The boundary conditions in the solution/crystal interfaces used the heat balance equation and mass balance equation.

To relate these equations, the liquidus curve in the InSb–GaSb pseudo-binary phase diagram was used. The governing equations and the associated boundary conditions were transformed to non-dimensional
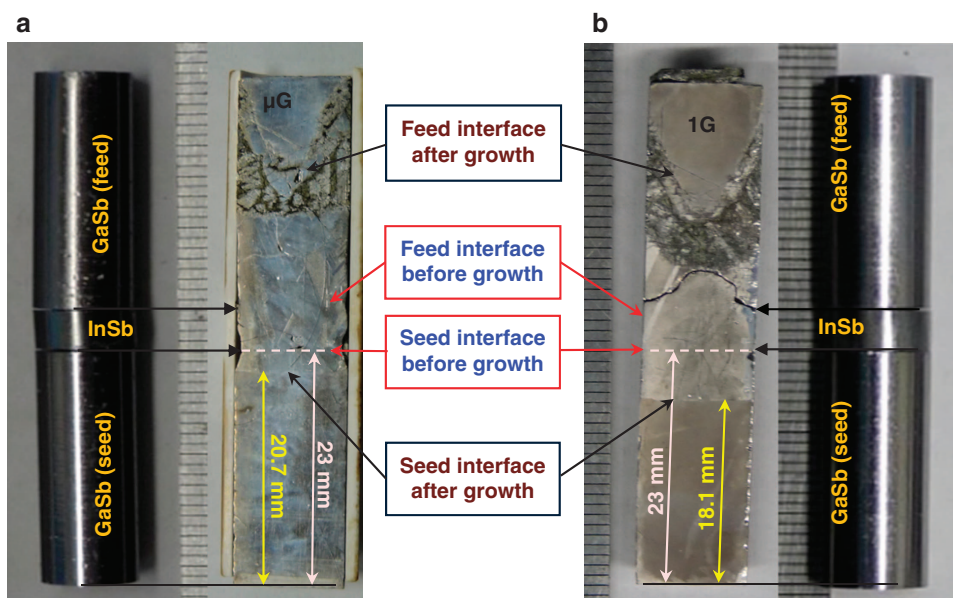

Figure 1. Schematic diagram of the vertical temperature profile (**a**), initial stage of sandwich sample (**b**), dissolution (**c**) and growth process (**d**) of the vertical gradient freezing method that was employed for the crystal growth.

Figure 2. Sandwich samples before and after experiments (**a**) under μG and (**b**) 1G. The interface positions of μG (**a**) and 1G samples (**b**) before and after the experiments are indicated.
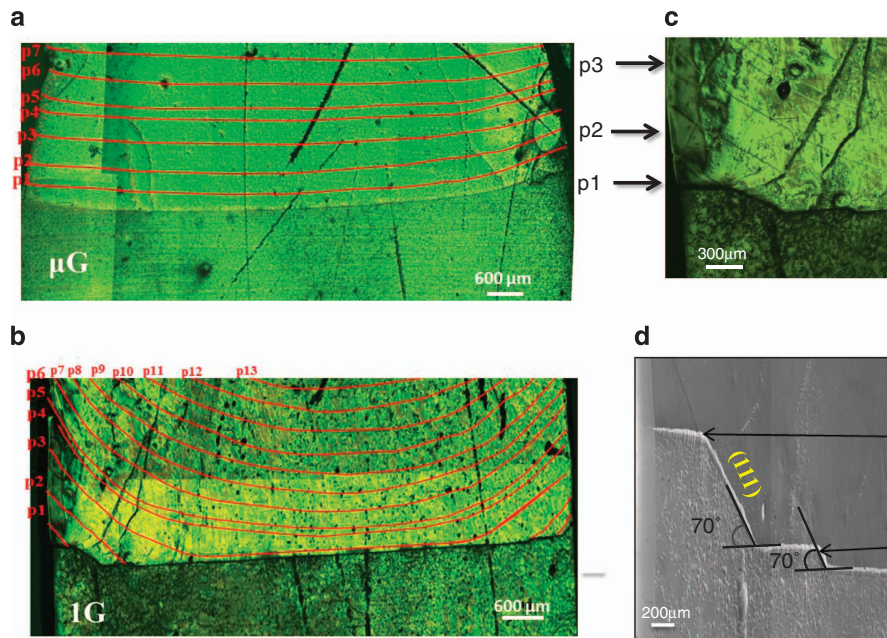
Figure 3. Polarized optical microscope images of the etched surfaces of (**a**) µG and (**b**) 1G samples. (**c**) Optical micrograph and (**d**) field emission scanning electron microscopy image of the periphery of the 1G sample. The striations are marked as p1, p2 and p3 in (**c**).

equations, and the boundary fixing method was adapted to the equations to handle the difficulties associated with curved interfaces. These equations were solved using the finite-volume method.

RESULTS

Figure 2a, b shows the cross section of µG and 1G samples. The dissolution lengths of GaSb seed and feed crystals under µG were 2.3 and 15 mm, respectively, whereas they were 4.9 and 11 mm in the 1G sample. The dissolution length of the seed crystal was larger in the 1G sample, whereas the dissolution length of the feed crystal was larger in the µG sample. The strong convection in the solution causes a large amount of seed dissolution under 1G, whereas under µG, the solute transport was diffusion dominant, decreasing the seed dissolution rate, as confirmed by our numerical simulation results.[28] The length of the crystal grown under µG (14.9 mm) was larger than that of the 1G sample (12.6 mm) because a larger amount of feed was supplied for growth under diffusive transport compared with the 1G experiment. The shape of the un-dissolved feed interface was similar for both samples, which ensured the same temperature distribution during both experiments. Figure 3a–c shows an optical micrograph of the un-dissolved seed interface of µG and 1G samples. As can be seen from Figure 3a, the interface shape of the µG sample was slightly concave toward the seed end and symmetric. However, the interface shape of the 1G sample was nearly flat with steps at the peripheries (Figure 3b, c). Moreover, the angles of steps 1 and 2 (Figure 3d) are around 70°, which confirmed that both steps were in the (111) plane. This shows that the kinetics played a more dominant role in the dissolution process under 1G when compared with µG.

The shapes of striations near the seed interface in µG and 1G samples are shown in Figure 3a, b. For clarity, the striations are marked as solid lines in the optical microscopic images of the etched samples. The striations formed by their corresponding heat pulses were marked as p1, p2 and so on. Initially, the growth started at the peripheries in the 1G samples, as striations 1 and 2 were observed at the peripheries and disappeared at the center (marked as p1 and p2 in Figure 3c). The initial striations were clearly observed at the center and periphery of the µG sample,

and the shape of the striations resembled the interface shape, which indicated a flat interface (Figure 3a). In the 1G sample, the striations were highly concave, while the initial seed interface was nearly flat, with steps at the peripheries. Figure 4a and b shows the EPMA mapping of indium distribution in the µG and 1G samples. The magnified images of indium mapping at the seed and feed interfaces of both samples illustrate the variations of interface shape at the initial and final stages of growth under µG and 1G. From the mapping, it is clear that the shape of the growth interface of the µG sample remained almost the same from the initial to the final stage of growth (Figure 4a). However, the growth interface of the 1G sample was nearly flat at the initial stage and highly concave toward the feed at the final stage of growth, as shown in Figure 4b. Moreover, a 'V'-shaped feed interface was observed in both samples beyond the residual solution region. To ascertain the quality of the grown crystals, the etch pit variations in crystals grown under µG and 1G were comparatively analyzed. Figure 5a, b shows optical micrographs of the etched surfaces of µG and 1G samples. The etch pit density (EPD) was calculated by counting the pits in both samples with respect to seed and grown crystals. The EPD was higher for the seed crystals in both samples because the seed crystals are grown by the Czochralski method at high temperature. The EPD was lower in the grown crystal under µG (2.16×10^4/cm^2) compared with that grown under 1G (2.72×10^4 /cm^2).

DISCUSSION

The strong convection and vortex at the center causes the solute transport from the center to the periphery under 1G. The velocity of the vortex flow is relatively low at the peripheries; thus, the dissolution is smaller at the peripheries. Moreover, the solutes accumulate at the peripheries while the solution at the center remains undersaturated because of strong convection. Therefore, the solution at the peripheries becomes supersaturated and the growth is initiated at the peripheries under 1G. Under µG, the solute transport is diffusion dominant; the solute is evenly transported from feed to seed, the solution attains equilibrium at the seed interface, and growth is initiated at the peripheries and center at nearly the same time. The growth was initiated faster
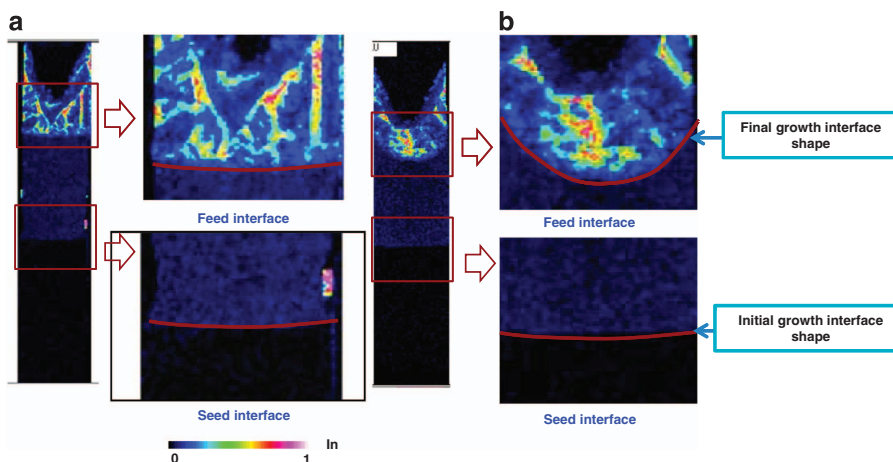
Figure 4. Electron probe micro analysis mapping of indium distribution in the (**a**) μG and (**b**) 1G samples. The magnified seed and feed interfaces of both samples illustrate the variations of the interface shape at the initial and final stages of growth under μG and 1G.
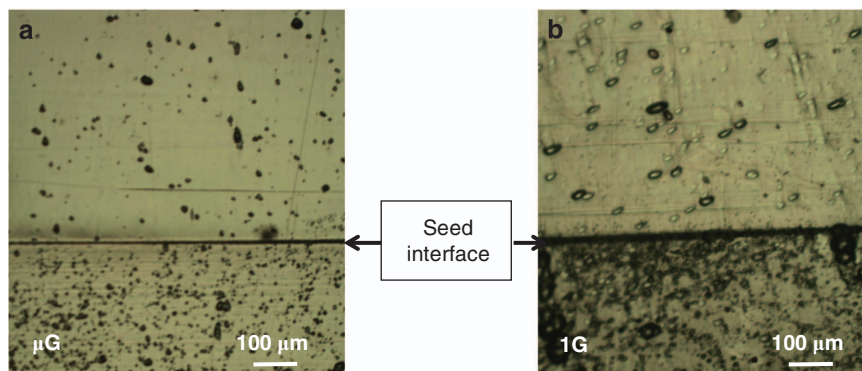

Figure 5. Optical microscope images of the etched surfaces of (**a**) μG and (**b**) 1G samples. The arrow shows the position of seed interface between GaSb and InGaSb crystals. The etch pits are shown as white arrows in the images.
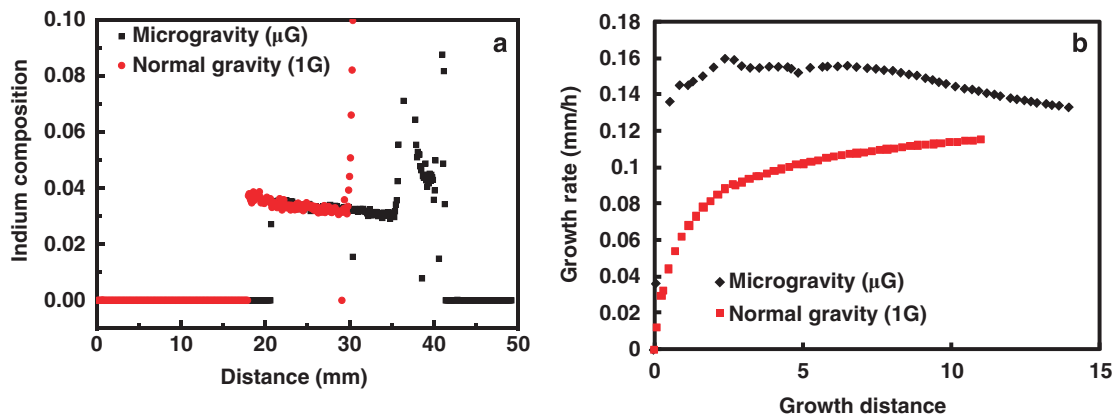

Figure 6. (**a**) Indium composition profile of μG and 1G samples and (**b**) growth rate variations of μG and 1G samples.

under μG compared to 1G, as all the striations were observed in the crystals (Figure 3a), possibly because of the absence of solutal convection. In the 1G sample, the growth was delayed because of the presence of convection, which hinders the solution from attaining equilibrium. As a result, the initial striations were not observed at the center of the sample (Figure 3b). The solution exhibits two kinds of flows resulting from compositional and temperature variations in the solution. One is the dominant convective flow in the middle region from seed to feed interface that returns to seed interface through the periphery. Another weak flow is at the periphery region from the seed to feed interface that returns to the seed interface through the middle. As

time elapses, the flow at the periphery region is suppressed by the flow from the central region. Therefore, higher amounts of solutes are accumulated at the peripheries. As a consequence, the solution at the periphery becomes supersaturated, leading to the initiation of growth under 1G condition.

The composition profile of the crystals was measured along the growth direction, as shown in Figure 6a. The composition profile clearly indicates that In$_x$Ga$_{1-x}$Sb crystal grew under μG from 20.2 to 35.1 mm; thus, the length of the grown crystal was 14.9 mm. However, the crystal grew under 1G from 18.0 to 30.6 mm, with a grown length of 12.6 mm. As can be seen from Figures 2a, b and 6a, approximately 2.3 and 4.9 mm of GaSb seed was dissolved into the InSb melt under μG and 1G, respectively. The amount of indium gradually decreased along the growth direction and fluctuated after 35.1 and 30.6 mm in μG and 1G samples, respectively. Because the crystal cooled after the growth period, the residual solution rapidly solidified, which caused the compositional fluctuation at the end of growth. As growth proceeds, the growth interface moves towards the high-temperature region, leading to a gradual increase in growth temperature in accordance with the temperature gradient. As a result, the relative amount of indium decreased along the grown length. The indium composition of the μG sample at the seed interface was 0.028 and gradually decreased along the growth direction. The indium composition of the 1G sample at the seed interface was 0.041 because of the large amount of seed dissolution, which shifted the interface position towards the low-temperature seed end. The EPMA mapping of the samples (Figure 4a) illustrates the homogeneous distribution of indium in the grown region. Moreover, the indium composition data were converted to growth temperature using an InSb–GaSb binary phase diagram, and the temperature gradient was calculated. The calculated temperature gradient of the μG sample (0.64 °C/mm) was slightly lower than that of the 1G sample (0.58 °C/mm), and the calculated values were almost the same as that fixed during the growth.

By measuring the grown length between the striations, the growth rates of the crystals were determined. Figure 6b shows the growth rate variation along the growth direction of μG and 1G samples. The growth rate of the crystal under μG was higher than that under 1G. The growth rate of the μG sample was 0.135 mm/h at 0.5 mm of grown length, increasing to a maximum of 0.16 mm/h when the grown length reached 2.4 mm, and the growth rate became stable after the grown length of 3 mm. The diffusion-controlled steady-state growth continued for the next 6 mm of grown length. Under 1G, the initial growth rate was one order of magnitude lower than that under μG, as a rate of 0.04 mm/h was measured at 0.5 mm of grown length of the 1G sample. The maximum growth rate of 0.11 mm/h was observed at 7.8 mm of grown length, and the diffusion-controlled steady-state growth period was only a few mm at the final stage of growth because of the strong convection under 1G.

Under μG the solutes dissolved at the seed interface were not able to move up to the feed interface unlike the 1G condition, due to the absence of convection, and thus the solution at the seed interface gets locally supersaturated. Therefore, under μG, the growth started earlier than 1G condition. Moreover, the dissolved solutes from feed interface sturdily diffuse towards seed interfaces due to density gradient between the solute and solvent. Therefore, the growth rate is relatively high under μG compared to 1G. On the contrary, under 1G, convection is dominant, which reduced the solute accumulation near the seed interface. Moreover, seed dissolution is stopped once crystal starts to grow from the seed interface. Hence the initiation of growth was delayed and growth rate is low compared to μG.

In$_x$Ga$_{1-x}$Sb alloy crystal was grown under μG at the ISS using a GaSb (111)A/Te-doped InSb/GaSb (111)A sandwich sample using a vertical gradient freezing method. A similar experiment was conducted under 1G on Earth. The dissolution and growth processes of μG and 1G samples were comparatively analyzed. The kinetics played a dominant role in the dissolution process under 1G, as steps were observed at the peripheries of the seed interface. The seed interface of the μG sample was highly symmetric and slightly concave. The growth started at the peripheries under 1G, which can be explained using the calculated flow velocity of the solution at high temperature. The growth rate was higher under μG compared with 1G. The quality of the μG sample was better, as low EPD was observed compared with the 1G sample. The suppressed convection under μG affected the dissolution and growth process of this alloy semiconductor.

CONTRIBUTIONS

Y.I., Y.H. and Y.O. designed and carried out the μG experiments. M.A., G.R., V.N.K., T.K., Y.M., T.O. and Y.H. prepared the ampoules and performed the crystal growth under normal gravity. Y.O. calculated the convective flow velocities by numerical simulation. M.A., V.N.K., Y.H., Y.I. and K.S. measured the composition of the crystal and analyzed the grown samples.

COMPETING INTERESTS

The authors declare no conflict of interest.

REFERENCES

1 Dutta PS, Bhat HL, Vikram K. The physics and technology of gallium antimonide: an emerging optoelectronic material. *J Appl Phys* 1997; **81**: 5821–5870.
2 Refaat TE, Abedin MN, Bhagwat V, Bhat IB, Dutta PS, Singh UN. InGaSb photo-detectors using an InGaSb substrate for 2 μm applications. *Appl Phys Lett* 2004; **85**: 1874–1876.
3 Xia L, Boos JB, Bennett BR, Ancona MG, del Alamo JA. Hole mobility enhancement in In$_{0.41}$Ga$_{0.59}$Sb quantum-well field-effect transistors. *Appl Phys Lett* 2011; **98**: 053505.
4 Takei K, Madsen M, Fang H, Kapadia R, Chuang S, Kim HS et al. Nanoscale InGaSb heterostructure membranes on Si substrates for high hole mobility transistors. *Nano Lett* 2012; **12**: 2060–2066.
5 Paskov PP. Refractive indices of InSb, InAs, GaSb, InAsSb and InGaSb: effects of free carriers. *J Appl Phys* 1997; **81**: 1890–1898.
6 Blom GM, Plaskett TS. The In-Ga-Sb ternary phase diagram. *J Electrochem Soc: Solid State Sci.* 1971; **118**: 1831–1833.
7 Kim KM. Morphological instability under constitutional supercooling during the crystal growth of InSb from the melt under stabilizing thermal gradient. *J Cryst Growth* 1978; **44**: 403–413.
8 Chen NF, Zhong X, Lin L. Comparison of field effect characteristics between space-grown and earth-grown gallium arsenide single crystal substrates. *Appl Phys Lett* 2001; **78**: 478–479.
9 Snell EH, Judge RA, Crawford L, Forsythe EL, Pusey ML, Sportiello M et al. Investigating the effect of impurities on macromolecule crystal growth in microgravity. *Cryst Growth Des* 2001; **2**: 161–168.
10 Editorial Notes. Space materials research: hanging by a thread. *Nature Mater.* 2004; **3**: 837.
11 Kundrot CE, Judge RA, Pusey ML, Snell EH. Microgravity and macromolecular crystallography. *Cryst Growth Design* 2001; **1**: 87–99.
12 Nakamura T, Nishinaga T. Distribution of Te in GaSb grown by Bridgman technique under μG. *J Cryst Growth* 2000; **211**: 434–440.
13 Benz KW. Crystal growth under reduced gravity. *Prog Cryst Growth Charact* 1993; **26**: 267–284.

6

14 Nishinaga T, Ge P, Huo C, He J, Nakamura T. Melt growth of striation and etch pit free GaSb under microgravity. *J Cryst Growth* 1997; **174**: 96–100.

15 Duffar T, Serrano MD, Moore CD, Camassel J, Contreras S, Dusserre P *et al.* Bridgman solidification of GaSb in space. *J Cryst Growth* 1998; **192**: 63–72.

16 Kinoshita K, Ogata Y, Adachi S, Yoda S, Tsuru T, Miyata H *et al.* Growth of a Si$_{0.50}$Ge$_{0.50}$ crystal by the traveling liquidus-zone (TLZ) method in microgravity. *J Cryst Growth* 2014; **192**: 12–16.

17 Murdoch N, Rozitis B, Nordstrom K, Green SF, Michel P, de Lophem TL *et al.* Granular convection in microgravity. *Phys Rev Lett* 2013; **110**: 018307.

18 Egry I, Lohoefer G, Jacobs G. Surface tension of liquid metals: results from measurements on ground and in space. *Phys Rev Lett* 1995; **75**: 4043–4046.

19 Glicksman ME, Koss MB. Dendritic growth velocities in microgravity. *Phys Rev Lett* 1994; **73**: 573–576.

20 Chathoth SM, Damaschke B, Samwer K, Schneider S. Thermophysical properties of Si, Ge and Si-Ge alloy melts measured under microgravity. *Appl Phys Lett* 2008; **93**: 071902.

21 Oprisan A, Oprisan SA. Universality in early-stage growth of phase-separating domains near the critical point. *Phys Rev E* 2008; **77**: 051118.

22 Okitsu K, Hayakawa Y, Yamaguchi T, Hirata A, Fujiwara S, Okano Y *et al.* Melt mixing of the 0.3In/0.7GaSb/0.3Sb solid combination by diffusion under microgravity. *Jpn J Appl Phys* 1997; **36**: 3613–3619.

23 Hayakawa Y, Balakrishnan K, Komatsu H, Murakami N, Nakamura T, Koyama T *et al.* Drop experiments on crystallization of InGaSb semiconductor. *J Cryst Growth* 2002; **237-239**: 1831–1834.

24 Hayakawa Y, Okano Y, Hirata A, Imaishi N, Kumagiri Y, Zhong X *et al.* Experimental and numerical investigations on dissolution and recrystallization processes of GaSb/InSb/GaSb under microgravity and terrestrial conditions. *J Cryst Growth* 2000; **213**: 40–50.

25 Okano Y, Umemura S, Enomoto Y, Hayakawa Y, Kumagawa M, Hirata A *et al.* Numerical study of Marangoni convection effect on the melting of GaSb/InSb/GaSb. *J Cryst Growth* 2002; **235**: 135–139.

26 Hayakawa Y, Balalaishnan K, Komatsu H, Murakami N, Nakamura T, Koyama T. Microgravity experiments on melting and crystallization of InGaSb. *Acta Astronaut.* 2002; **51**: 221–227.

27 Rajesh G, Arivanandhan M, Morii H, Aoki T, Koyama T, Momose Y *et al.* In-situ observations of dissolution process of GaSb into InSb melt by X-ray penetration method. *J Cryst Growth* 2010; **312**: 2677–2682.

28 Rajesh G, Arivanandhan M, Suzuki N, Tanaka A, Morii H, Aoki T *et al.* Effects of solutal convection on the dissolution of GaSb into InSb melt and solute transport mechanism in InGaSb solution: numerical simulations and in-situ observation experiments. *J Cryst Growth* 2011; **324**: 157–162.

29 Arivanandhan M, Rajesh G, Koyama T, Momose Y, Sanakaranarayanan K, Tanaka A *et al.* Crystal growth of InGaSb alloy semiconductor at international space station: reliminary experiments. *J Jpn Soc Microgravity Appl* 2011; **28**: s46–s50.

30 Arivanandhan M, Rajesh G, Tanaka A, Ozawa T, Okano Y, Inatomi Y *et al.* Bulk growth of InGaSb alloy semiconductor under terrestrial conditions: a preliminary study for microgravity experiments at ISS. *Defect Diffus Forum* 2012; **323–325**: 539–544.

31 Sakata K, Mukai M, Rajesh G, Arivanandhan M, Inatomi Y, Ishikawa T *et al.* Thermal properties of molten InSb, GaSb, and In$_x$Ga$_{1-x}$Sb alloy semiconductor materials in preparation for crystal growth experiments on the international space station. *Adv Space Res* 2014; **53**: 689–695.